












A glimpse into the fungal metabolomic abyss: Novel network analysis reveals relationships between exogenous compounds and their outputs

Muralikrishnan Gopalakrishnan Meena ^{a,*1}, Matthew J. Lane ^{b,c,1}, Joanna Tannous^b, Alyssa A. Carrell^b, Paul E. Abraham ^b, Richard J. Giannone ^b, Jean-Michel Ané ^{d,e}, Nancy P. Keller ^{d,f}, Jesse L. Labbé ^{b,g}, Armin G. Geiger ^{b,c}, David Kainer ^{b,h}, Daniel A. Jacobson ^b and Tomás A. Rush ^{b,*}

^aNational Center for Computational Sciences, Oak Ridge National Laboratory, Oak Ridge, TN 37831, USA

^bBiosciences Division, Oak Ridge National Laboratory, Oak Ridge, TN 37831, USA

^cBredesen Center for Interdisciplinary Research and Graduate Education, University of Tennessee, Knoxville, TN 37916, USA

^dDepartment of Bacteriology, University of Wisconsin-Madison, Madison, WI 53706, USA

^eDepartment of Agronomy, University of Wisconsin-Madison, Madison, WI 53706, USA

^fDepartment of Medical Microbiology and Immunology, University of Wisconsin-Madison, Madison, WI 53706, USA

^gNow at Tekholding, Salt Lake City, UT 84119, USA

^hNow at ARC Centre of Excellence for Plant Success in Nature and Agriculture, University of Queensland, Brisbane, QLD 4072, Australia

*To whom correspondence should be addressed: Email: gopalakrishm@ornl.gov (M.G.M.); rushta@ornl.gov (T.A.R.)

¹These authors contributed equally to this work.

Edited By: Li-Jun Ma

Abstract

Fungal specialized metabolites are a major source of beneficial compounds that are routinely isolated, characterized, and manufactured as pharmaceuticals, agrochemical agents, and industrial chemicals. The production of these metabolites is encoded by biosynthetic gene clusters that are often silent under standard growth conditions. There are limited resources for characterizing the direct link between abiotic stimuli and metabolite production. Herein, we introduce a network analysis-based, data-driven algorithm comprising two routes to characterize the production of specialized fungal metabolites triggered by different exogenous compounds: the direct route and the auxiliary route. Both routes elucidate the influence of treatments on the production of specialized metabolites from experimental data. The direct route determines known and putative metabolites induced by treatments and provides additional insight over traditional comparison methods. The auxiliary route is specific for discovering unknown analytes, and further identification can be curated through online bioinformatic resources. We validated our algorithm by applying chitooligosaccharides and lipids at two different temperatures to the fungal pathogen *Aspergillus fumigatus*. After liquid chromatography–mass spectrometry quantification of significantly produced analytes, we used network centrality measures to rank the treatments' ability to elucidate these analytes and confirmed their identity through fragmentation patterns or in silico spiking with commercially available standards. Later, we examined the transcriptional regulation of these metabolites through real-time quantitative polymerase chain reaction. Our data-driven techniques can complement existing metabolomic network analysis by providing an approach to track the influence of any exogenous stimuli on metabolite production. Our experimental-based algorithm can overcome the bottlenecks in elucidating novel fungal compounds used in drug discovery.

Significance Statement

Triggering silent biosynthetic gene clusters in fungi to produce specialized metabolites is a tedious process that requires evaluating various environmental conditions by using epigenetic modulating agents or cocultures with other microbes. We present two data-driven approaches employing network analysis to elucidate specialized metabolite production by exogenous treatments. The direct route reveals the relationship between treatments and production of known/putative specialized metabolites, whereas the auxiliary route distinguishes unique unknown analytes from abundantly produced ones. Our predictions were validated by comparing them with fragmentation patterns or standards. These techniques enable researchers to identify treatments that could enhance targeted metabolite production or detect unique analytes, which can be further screened and characterized for their biological activities, facilitating the discovery of new metabolites.

Competing Interest: The authors declare no competing interest.

Received: July 19, 2023. **Accepted:** September 20, 2023

© The Author(s) 2023. Published by Oxford University Press on behalf of National Academy of Sciences. This is an Open Access article distributed under the terms of the Creative Commons Attribution-NonCommercial-NoDerivs licence (<https://creativecommons.org/licenses/by-nc-nd/4.0/>), which permits non-commercial reproduction and distribution of the work, in any medium, provided the original work is not altered or transformed in any way, and that the work is properly cited. For commercial re-use, please contact journals.permissions@oup.com

Introduction

Fungi are among the most prolific producers of specialized metabolites, which can be classified into five main classes by their chemical structure: polyketides, nonribosomal peptides, terpenes, indole alkaloids, and isocyanides (1–3). These specialized metabolites are multifaceted and impactful in our daily lives due to their positive roles in lifesaving drugs and agrochemicals. On the contrary, some of these specialized metabolites, commonly called mycotoxins, can have adverse effects on humans, animals, and crops and cause illnesses and economic losses (1, 4, 5). In fungi, the genes involved in the biosynthesis of specialized metabolites are commonly arranged in so-called biosynthetic gene clusters (BGCs). Many specialized metabolite BGCs have been predicted and identified from genomes of several filamentous fungi (1–3). However, most predicted metabolites cannot be produced under standard cultivation and growth conditions, thereby hindering their discovery (6). In recent years, the chance to expand our knowledge and repertoire of specialized metabolites has significantly increased owing to the enhanced understanding of fungal diversity and taxonomy, the widespread availability of published genomes (7, 8), and the development of BGC prediction tools (9) such as antiSMASH (10–12) and other computational tools (13–22). Biosynthetic genes predicted by these approaches can undergo genetic manipulations afterward to confirm their implication in the metabolic pathway and characterize novel specialized metabolites (23, 24). However, this approach can sometimes be challenging, mainly if the BGC is missing a specific transcription factor to genetically target or if the gene cluster's borders have been inaccurately predicted (25). With the ongoing challenges of triggering those silent BGCs for specialized metabolite characterization, other approaches have been proposed.

The recently adopted approaches to trigger the expression of uncharacterized BGCs relied on identifying environmental cues, epigenetic chemical factors, axenic cultivation conditions, applications of exogenous compounds, or cocultivation of the fungus with other microbes or hosts to induce the production of corresponding metabolites (1, 2, 6, 9, 26–28). To interpret how these abiotic or biotic triggers induce metabolite production, network analysis (29) has been proposed as a complementary approach to accurately predict the factors that can elucidate fungal metabolites and narrow down the list of BGCs to target (25, 30). Various state-of-the-art techniques can help discover new specialized metabolites through network analysis, artificial intelligence, and data-driven approaches, such as using molecular network analysis for web-based servers such as GNPS (21, 22), MetWork (13), and MetaboAnalyst (31, 32). These web servers perform a variety of data-driven analyses on mass spectrometry data to discover new metabolites and characterize the structure of known and putative metabolites. Molecular networks are built using spectral matching [spectral network analysis (33)] to discover unknown compounds. However, to our knowledge, there are no tools developed to assess the direct effect of exogenous treatments on the production of fungal specialized metabolites. Thus, there is currently a knowledge gap regarding the sources that trigger the production of such specialized metabolites.

The goal of the work described here is to determine the feasibility of using network analysis to track the influence of applied exogenous compounds on the production of characterized and putative metabolites as well as unknown analytes. We introduce two methods based on network analysis to tackle these two objectives: *direct route* and *auxiliary route*. An overview of the modeling framework is shown in Fig. 1 with suggestions of postanalysis

applications. The direct route shows the influence of treatments on the production of known or putative specialized metabolites. In contrast, the auxiliary route distinguishes unique unknown analytes and pinpoints the treatments that foster their production. Both approaches reveal treatments that dominate by triggering a variety of specialized metabolites. Moreover, unique specialized metabolites are also identified by these methods. The capability of these methods was evaluated using the opportunistic human pathogen and soilborne saprotroph *Aspergillus fumigatus* as a model organism exposed to various chitoooligosaccharides (COs) and lipid treatments.

The objective of the current study is not to discover new metabolites. However, further studies using these methods could lead to the identification of novel metabolites but would require to the postanalysis methods shown in Fig. 1. Our goal is to reveal the effect of exogenous treatments on triggering the production of specialized metabolites. Nonetheless, the inferences drawn on the dominant treatments and unique specialized metabolites using the current methodology can enable the discovery of new metabolites through the suggested postanalysis applications in Fig. 1 (top-right box). The developed methods can complement existing web-based network analysis tools (13, 21, 22, 31, 32) used for metabolite discovery that do not consider the sources that trigger metabolomic outputs and have application potential in various fields, including drug discovery and development.

Framework to provide data-driven network analysis

Methodology: building bipartite networks of treatments and metabolomic outputs

Bipartite networks are built to quantify the relationship between metabolites and the sources that trigger their production, such as exogenous biomolecules or compounds. A network (or graph) is a collection of nodes connected by lines called *edges*. The nodes represent the entities or elements of a system, and the edges represent the interaction or relationship among the features (29, 34). For example, in cell metabolism, a metabolic network represents the biochemical reactions among substrates that result in products (29, 35, 36). The nodes of the metabolic network represent the substrates, and the edges represent the metabolic reactions among the substrates. In the current analysis, we assessed the effect of exogenous compounds on the production of specialized microbial metabolites. This relationship between exogenous treatments and specialized metabolites can be represented by a network, as shown in Fig. 1. The nodes can be classified into two types: (1) the treatments and (2) the specialized metabolites that result in a bipartite network. The edges represent the magnitude of up- or downregulation of specialized metabolites caused by the treatments compared to a controlled case (measured by the magnitude of a \log_2 fold change using processed spectral data from targeted liquid chromatography–mass spectrometry [LC-MS] analysis). The sign of regulation can also be incorporated into the network definition, thereby leading to signed networks. In this pilot study, we only use the magnitude of the regulation value to reveal the effect of the exogenous treatments on triggering metabolite production. The signed network can indeed extract the specific trigger (e.g. up- or downregulation) of the treatments, and this will be addressed in future work. The details of building the bipartite network are provided in [Online Supplementary Material A](#).

The bipartite network provides an in-depth quantification and clear visual representation of a treatment's ability to

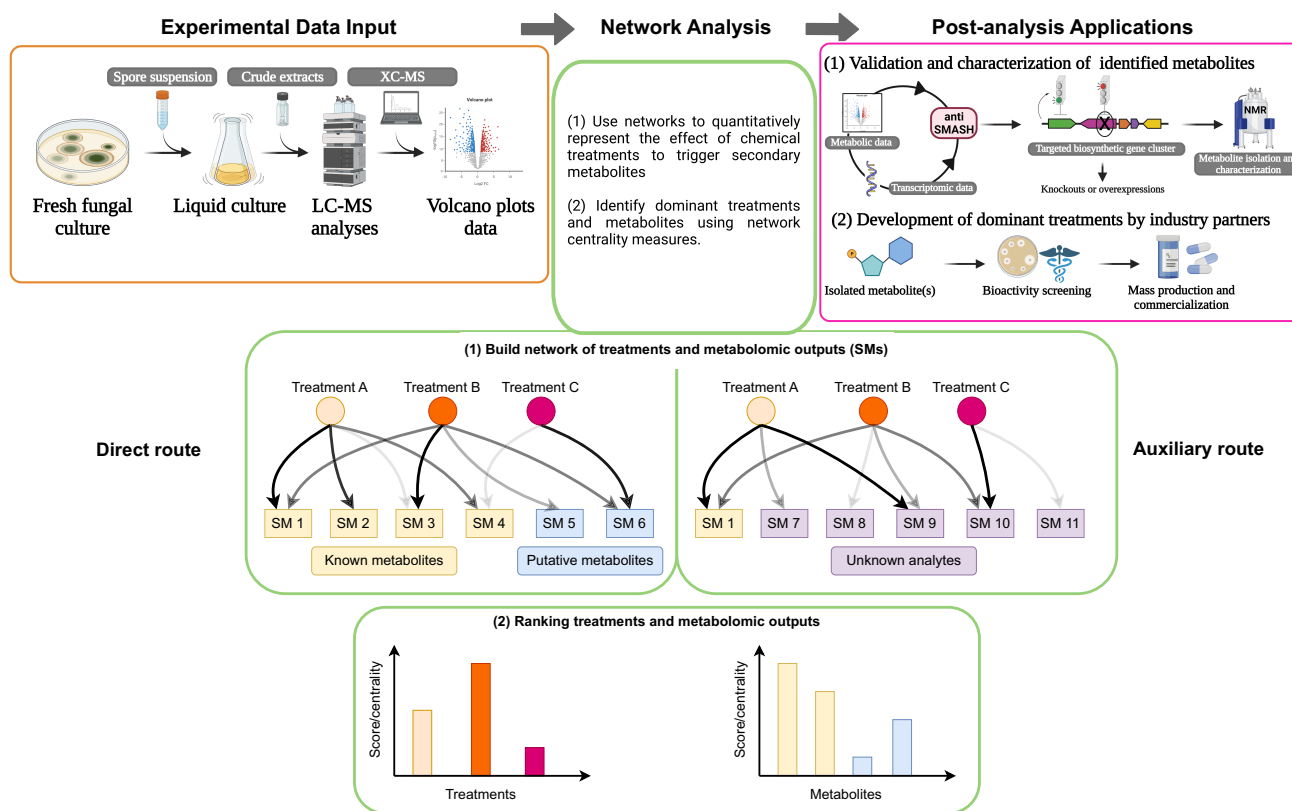


Fig. 1. Framework of the direct and auxiliary routes using experimental inputs and implications for postanalysis applications. An overview of the network analysis approach reveals the effect of exogenous compounds on triggering the production of microbial specialized metabolites. In our experimental design, the data are obtained after exposing *A. fumigatus* to various abiotic or biotic factors for specific time points. The fungal exudates are separated from the fungal biomass, extracted through a filter membrane, homogenized with an organic solvent (ethyl acetate), and separated from the aqueous phase, dried, and resuspended in acetonitrile and water (50:50) (v/v). These samples were later processed through ultra-high pressure liquid chromatography-mass spectrometry (UHPLC-MS), which provides spectra data. Next, the spectra data are analyzed through XCMS and curated to retain only significant analytes with a P -value < 0.05 and a \log_2 fold change > 1.0 or < -1.0 . The data are represented in volcano plots, which is standard practice to display differences of metabolite production between treated samples and the control. To develop our novel method, we used the \log_2 fold change data points for the network analysis that quantitatively represent the effect of exogenous treatments to trigger specialized metabolites. The treatments and metabolomic outputs are ranked by using network analysis measures through our two new methods: the direct route and the auxiliary route. The direct route is used to understand the influence of treatment on known or putative metabolites. MAVEN was used to identify and match the peak intensity, m/z , and retention time of known or putative metabolites previously described or predicted in *A. fumigatus*. Known metabolites were also confirmed through fragmentation patterns or in silico spiking with a commercial standard. Because spectra data can have baseline creeping, which causes peak noise and could influence the peak intensity, we further curated the spectra data to eliminate these artifacts to develop the auxiliary route. This route is used to identify strong signals of unknown analytes and screen with public databases such as KEGG or Lipid Maps to find known metabolites from other organisms that have not been described in *A. fumigatus*. After knowing the relationship between a treatment and metabolomic outputs, postanalysis applications can be applied to isolate and characterize the metabolite through genetic manipulations followed by bioactivity screening. These two postanalysis applications are provided as guidance on possible applications of the current framework for discovering new metabolites and are not performed in the current study.

trigger the production of various specialized metabolites. In this study, we provide two routes to assess specialized metabolite production by using the bipartite network formulation, as shown in Fig. 1. The first is the direct route to determine the bio-synthesis of known and putative metabolites, and the second is the auxiliary route to assess the production of unknown analytes or identify known metabolites not previously described in *A. fumigatus*. In the direct route, the network nodes include treatments that elucidate known and putative metabolites from a microbe. Moreover, we use network centrality measurements to rank the treatments and the specialized metabolites. Those measurements are used to identify the most influential nodes in a network (29). Herein, we used the centrality measurements of node strength and PageRank (37) to identify the most effective treatments and metabolites. The treatments are ranked based on their ability to trigger metabolite production, and the

metabolites are classified based on their popularity in being activated by various treatments. We provide details of computing the network centrality measures in [Online Supplementary Material A](#). In the auxiliary route, we build bipartite networks by using novel analyte peaks extracted from postprocessed spectral data. Furthermore, we analyze the network edges and neighbors of nodes to distinguish unique analytes among the total pool. Methods for novel peak selection are provided in [Online Supplementary Material A](#). Notably, the only similarity between the two routes is on the definition of the graphs/networks. Both routes involve bipartite networks defined by the amount of up- or downregulation of the specialized metabolites by the exogenous treatments. The preprocessing data curation and network centrality measures used to identify important specialized metabolites and treatments in each of the routes are different.

System: experimental data of *A. fumigatus* metabolomic outputs

Our modeling framework was used to reveal the effect of various COs and lipid treatments on triggering the production of specialized metabolites in *A. fumigatus*. Various COs and lipids were applied as exogenous treatments because they are common constituents found in most fungi (38–40). Moreover, lipids have been shown to influence fungal metabolomics (41); however, the impacts of COs remain unknown. In contrast, COs have antifungal activity (42), which could influence the metabolomic profile in *Aspergillus* species (27). We applied the treatments to the Af293 *A. fumigatus* strain because it has a well-defined repertoire of known and putative specialized metabolites (43) that are temperature-dependent (26, 27, 44–46); moreover, its entire genome has been sequenced (47). We also explored the influence of temperature on the production of specialized metabolites by conducting the experiments at 25 and 37°C. *A. fumigatus* is generally examined at 25°C to explore the extent of its metabolomic capabilities or its lifestyle as a soilborne saprotroph that recycles environmental carbon and nitrogen (48). However, the fungus is also an opportunistic human pathogen and is commonly examined at 37°C for its ability to cause aspergillosis, a lung disease found in immunocompromised patients (49). The details of the experimental setups and data generation are provided in [Online Supplementary Material A](#).

Results

Analyte and metabolomic production induced by treatments

Results at 25°C

To interpret and understand the produced analytes and metabolites, we used UpSet plots (Fig. 2a) and volcano plots (Fig. 2b–f) to interpret and understand the produced analytes and metabolites. The data curation for the UpSet plots (Fig. 2a for 25°C results and Fig. 3a for 37°C results) and volcano plots (Fig. 2b–f for 25°C results and Fig. 3b–f for 37°C results) was obtained by using the experimental results involving XCMS (15) to provide a statistical assessment of signals with significant peaks between a treatment and solvent control through a pairwise comparison. A list of mass to charge (m/z), retention times and statistical values were provided from those results (see [Online Supplementary Tables S1 and S2](#)). To validate the XCMS results, we used MAVEN (14, 20) for metabolomic analysis and visualization of the LC-MS data to confirm if the same m/z at the provided retention time did have a significant peak difference between treatment and solvent control.

At 25°C, LC-MS data revealed that all individually applied treatments significantly induced the production of analytes compared to the solvent control, as shown by the UpSet plot in Fig. 2a. No treatments were coapplied to the fungus. In total, 4,629 significant analytes were detected (Fig. 2a). Unique analytes produced by CO4 accounted for 15.5%, by CO5 11.4%, by CO8 3.7%, by palmitic acid 3.8%, and by oleic acid 12.5%. These results indicate that the length of COs largely influence specific metabolomic pathways. The shorter the CO chain, the higher was the production of analytes. In addition, oleic acid has a more significant impact on analyte production compared to palmitic acid. Interestingly, 38.3% of individual analytes were induced by CO4 and CO5, suggesting a common coregulation of metabolomic pathways. However, most analytes were uniquely caused by one treatment indicating that metabolomic pathways seem specific to treatment, thus requiring network analysis to determine those relationships.

To determine the regulation of analytes induced by treatment and identify potential known and putative specialized metabolites, we constructed volcano plots based on the \log_2 fold change and $-\log_{10}$ (P-values) between a treatment and the solvent control as shown in Fig. 2b–f. All treatments had a significant differential expression of analytes compared to the control. COs induce the production of analytes between 80 and 93% compared to the solvent control, including several known and putative metabolites (Fig. 2d–f). On the contrary, the positive regulation of analyte production by lipids was reduced compared to the control, ranging between 17 and 24%. CO4 (Fig. 2d) and CO5 treatments (Fig. 2e) induced the production of five to six known or putative metabolites, whereas CO8 (Fig. 2f) influenced the production of a single known metabolite. These results follow the same trend shown in Fig. 2a, highlighting that short-chain COs have a more significant impact on triggering metabolite production than long-chain CO. Interestingly, oleic acid (Fig. 2c) induced five times more known or putative metabolites than palmitic acid (Fig. 2b), matching the data shown in Fig. 2a. We also compared transcriptomic expression from quantitative PCR analysis to corrected peak area which show relatively similar regulation of known secondary metabolites ([Online Supplementary Fig. S2](#)). It is important to consider that specialized metabolomic production is potentially subject to post-transcriptional regulation when the transcriptomic and metabolomic data do not match. Discrepancies between metabolomic and transcriptomic profiles have been observed in other fungi (50).

Results at 37°C

We analyzed the LC-MS data with treated samples grown at 37°C, and this revealed that all individually applied treatments induce significant production of analytes compared with the solvent control, as shown by the UpSet plot in Fig. 3a. No treatments were coapplied to the fungus. As expected, the total number of analytes is lower at 37°C than at 25°C. In total, 1,807 significant analytes were detected (Fig. 3a). The percentage of unique analytes produced by CO4, CO5, CO8, palmitic acid, and oleic acid were 25.6, 13.6, 17.2, 10.6, and 5.0%, respectively. These results indicate that at 37°C, both short-chain and long-chain COs influence specific metabolomic pathways, unlike at 25°C. At 37°C, the CO8 treatment showed a higher production of specific metabolites by the fungus compared to 25°C. Contrary to what was observed at 25°C, oleic acid showed less influence on analyte production at 37°C compared with palmitic acid. Notably, most analytes were uniquely produced by a treatment rather than shared by multiple treatments at 37°C.

With the LC-MS data produced at 37°C, we constructed volcano plots based on the \log_2 fold change and $-\log_{10}$ (P-values) between a treatment and the solvent control, as shown in Fig. 3b–f. Although all treatments had a significant differential production of analytes compared with the solvent control at 37°C, it was less than that observed at 25°C, as expected (Fig. 2b–f). COs had a higher mean of abundance, ranging between 62 and 80% (Fig. 3d–f), whereas lipids had between 67 and 70% (Fig. 3b and c). These results mean that COs reduce the abundance of analytes at 37°C compared to 25°C. However, lipids showed a higher mean quantity of analytes at 37°C than at 25°C.

Summary of analyte and metabolomic production induced by treatments

In summary, short-chain COs and oleic acid have the most significant impact on known or putative metabolite and unknown

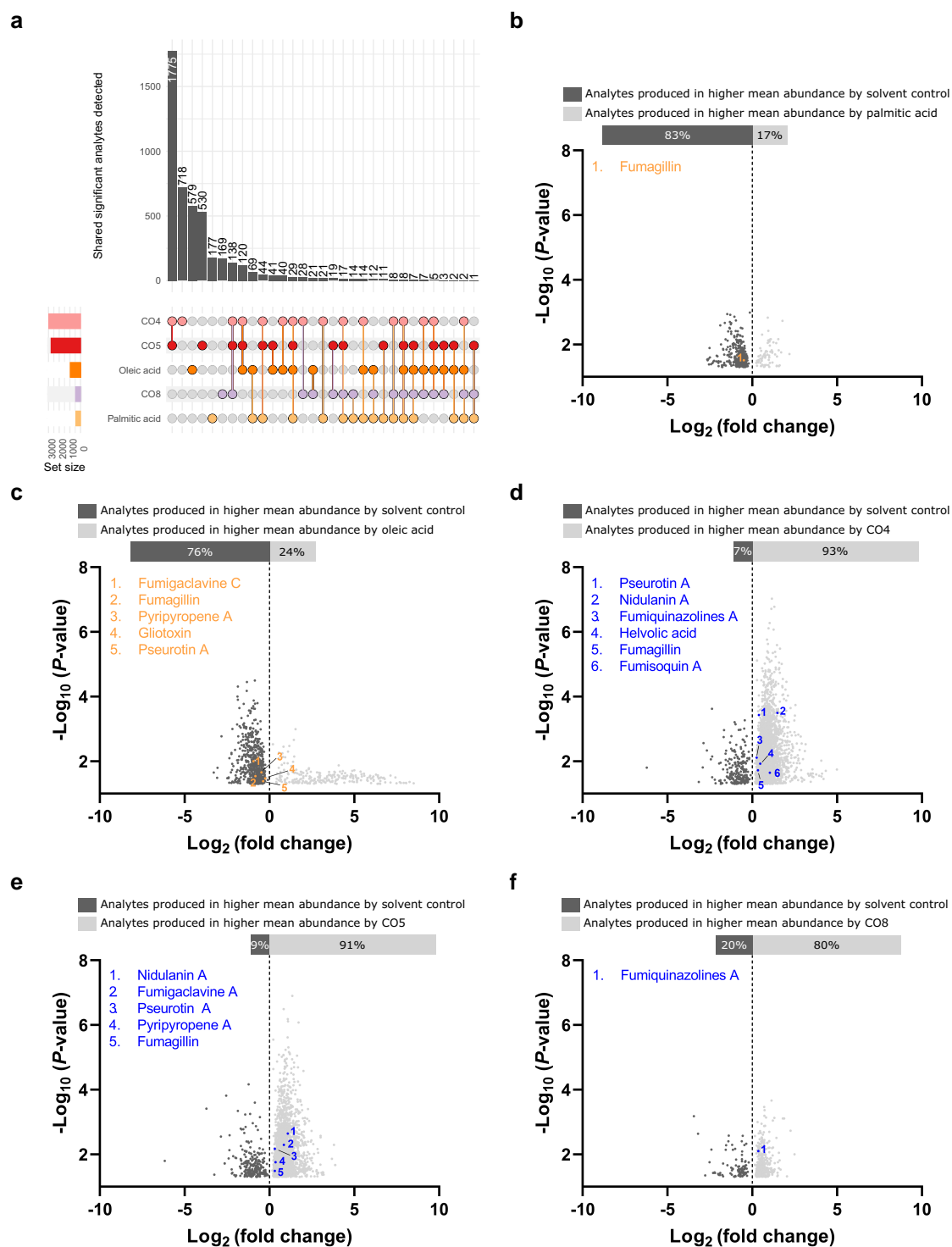


Fig. 2. Metabolomic outputs of *A. fumigatus* at 25°C induced by lipid and CO treatments. (a) UpSet plot denoting the number of significant analytes produced by individually applied treatments. Multiple treatments induced the same analytes. (b–f) Volcano plots identifying the known and putative metabolites and unknown analytes triggered by (b) palmitic acid, (c) oleic acid, (d) CO4, (e) CO5, and (f) CO8 compared with the solvent control.

analyte production at 25°C, yet they have different regulations at this temperature. The analyte and metabolomic production induced by the exogenous treatments, COs, and lipids is significantly different at both temperatures. The changes in these results indicate that treatments influence the production of analytes, but environmental cues like temperature also have significant effects. Therefore, further investigations to elucidate metabolites

should be conducted at 25°C for the CO treatments and 37°C for lipids. Interestingly, nearly all treatments increased the production of the same known or putative metabolites, fumiquinazolines F, fumigaclavine B, or pyripyropene A, whereas all treatments reduced the production of fumagillin at 37°C. The regulation of the latter compound was different at 25°C, at which the lipid treatments reduced its production, and the short-chain COs improved

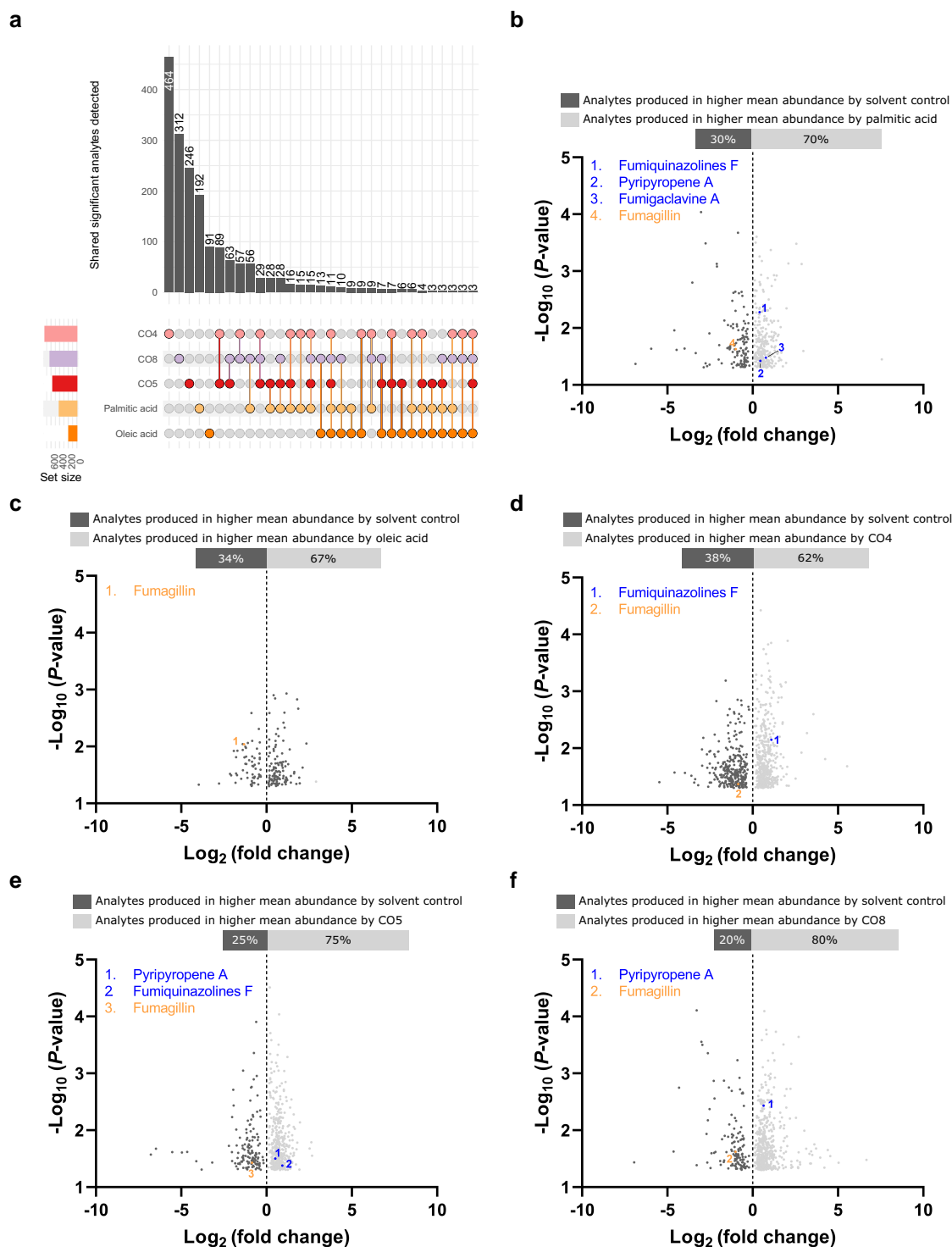


Fig. 3. Metabolomic outputs of *A. fumigatus* at 37°C induced by lipid and CO treatments. (a) UpSet plot denoting the number of significant analytes produced by individually applied treatments. Multiple treatments induced the same analytes. (b–f) Volcano plots identifying the known and putative metabolites and unknown analytes triggered by (b) palmitic acid, (c) oleic acid, (d) CO4, (e) CO5, and (f) CO8 as compared to the solvent control.

it. This indicates that lipids might be compounds that downregulate fumagillin production constantly across temperatures and could be further investigated as therapeutic molecules.

Traditional comparison charts or plots (e.g. UpSet plots, volcano plots) are typically used in an analysis to understand the differences between a control and a fungal metabolome subjected to treatment. Based on this data visualization and

identifying known secondary metabolites, studies could confirm their findings through fragmentation analysis and/or comparison to a commercial standard. In certain cases, gene characterization may be performed by employing knockout mutants. These standard practices do not provide answers on what treatments we should use for the upscaled production of a targeted, known metabolite or further characterization of an unknown metabolite.

Here, we present an alternative approach to delve deeper into interpreting the results with the direct and auxiliary routes, which are visually quantifiable approaches to demonstrate how multiple treatments influence multiple metabolites within a single diagram. First, we explore the direct route, which utilizes theoretical graph analysis to gain a more comprehensive understanding of the underlying regulatory mechanisms and the production of these metabolites within the system. Next, with the auxiliary route, we aim to putatively identify curated peaks to known metabolites from other organisms and determine if they are present in *A. fumigatus*. Last, we will confirm the identity of the predicted metabolites through fragmentation patterns or in silico spiking with a commercial standard.

Direct route reveals the dominant compounds and highly influenced known and putative metabolites

Results at 25°C

The influence of COs and lipids on the production of known and putative metabolites by *A. fumigatus* at 25°C was analyzed by using the direct route, as shown in Fig. 4a–c. The bipartite networks provide a visual representation and enable a clear distinction between the effects of these treatments (Fig. 4a). Although COs resulted in an upregulation of the identified metabolites, the lipids showed a downregulation. The network centrality measure of a node's out-strength (i.e. the size of the circles that represent treatment nodes in Fig. 4a) for the treatments reveals that CO4 has the highest effect on triggering metabolite production, followed by CO5 and then oleic acid. The CO8 and palmitic acid treatments showed minor influence for inducing metabolite production. This was expected because those two treatments influence the production of only one metabolite with low values of \log_2 fold change. The putative metabolite nidulanin A possesses the highest node in-strength (i.e. the size of the circles that represent metabolite nodes in Fig. 4a) among the metabolites because it is the most regulated metabolite. Among the known metabolites, fumagillin has the highest node in-strength, followed by pyripyropene A, pseurotin A, fumigaclavine A, and fumiquinazolines A. These metabolites seem to be highly upregulated by the CO4 and CO5, but downregulated by oleic acid. We demonstrate that the bipartite networks are an alternative way to visualize the results which are shown in the UpSet and volcano plots (Fig. 2a–f) as the node strength is simply the total \log_2 fold change values.

To further elucidate the important treatments and metabolites, we compute the network centrality measure of PageRank (Fig. 4b and c). PageRank considers various factors other than the total \log_2 fold change values to rank the nodes. These factors include the number of edges from or to a node and the relative importance of nodes based on their connections to highly and uniquely connected nodes. The ranking of the treatments by using the broadcasting PageRank values (Fig. 4b) shows that CO4 is the most effective treatment, closely followed by oleic acid and then CO5. For ranking the metabolites, we used the receiving PageRank measure (Fig. 4c), which shows that fumagillin is the most influenced metabolite, followed by fumiquinazolines A and then nidulanin A. A detailed comparison of PageRank values of the treatments and metabolites is provided in [Online Supplementary Material A](#). These results are counter intuitive compared to the UpSet and volcano plots. Below, we provide some insights into these differences and the advantage of using the direct route vs. traditional statistical tools such as UpSet and volcano plots.

Comparison of the direct route to traditional statistical methods with results produced at 25°C

The network analysis revealed the treatments that should be used to elucidate specific metabolites: CO4, oleic acid, and then CO5. If we only used UpSet and Volcano plots, we would conclude that treatments CO4, CO5, and then oleic acid should be used to elicit metabolite production. Interestingly, from this comparison, the set size between CO5 and oleic acid is different by roughly 50%. The difference between the data when using the direct route vs. the UpSet or Volcano plots is that the direct method shows the oleic acid has a more substantial influence on metabolite production, although it is not frequently shown in all data. CO5 influenced metabolite production in most conditions, but its influence was weaker than oleic acid. These results align with the inferences drawn from the UpSet and volcano plots in Fig. 2a–f. In both types of analysis, CO4 had the most extensive impact and was frequently shown in all conditions to be essential to elucidate secondary metabolite production. Regarding metabolite production, the direct route shows that fumagillin, fumiquinazolines A, and nidulanin A are the metabolites most influenced by CO4, CO5, and oleic acid treatments. If we solely relied on the traditional comparison charts, then a researcher might assume that pseurotin A and pyripyropene A are also critically influenced by our treatments. The direct route revealed that although these metabolites were detected in our analysis, their presence was weak. Instead, we see a strong correlation between our treatments and the production of fumagillin, fumiquinazolines A, and nidulanin A. Another interpretation of the data showed that CO8 and palmitic acid are poor treatments at this condition to elucidate these known metabolites. Additionally, helvolic acid and gliotoxin were detected in our samples. However, they were poorly produced regardless of the treatments used. To conclude, we demonstrate that all datasets should be considered, and although traditional methods show the frequency of producing a metabolite, the direct method shows the strength of that production and which treatment caused this production. Last, an example for further exploration from this dataset shows that if a researcher is interested in confirming if nidulanin A is genuinely produced by *A. fumigatus* (51), then the CO4 treatment can be used to induce a higher production of this putative metabolite and confirm it.

Results at 37°C

The direct route results reveal the treatments' influence on the production of specialized metabolites in *Aspergillus fumigatus* at 37°C (Fig. 5a–c). As expected, fewer analytes and known or putative specialized metabolites were produced at 37°C in both solvent controls and treatments, as shown in Fig. 5a and the UpSet plots in Fig. 3a. Furthermore, there is no clear distinction on how the two treatments regulate the production of metabolites. Both COs and lipids showed a positive and negative impact on metabolite production at 37°C, whereas COs upregulated the production of metabolites at 25°C, and lipids downregulated it (Fig. 4a). Notably, the metabolites fumagillin and pyripyropene A are the only metabolites that were uniquely and highly triggered at both temperatures; however, the treatments that started the production of these two metabolites were different depending on the temperature. The bipartite network representation further clarifies such pathways and regulations. With the limited number of data points, both the node strength and PageRank measures provide similar results for identifying the effective treatments and most receptive metabolites, as shown in Fig. 5b and c.

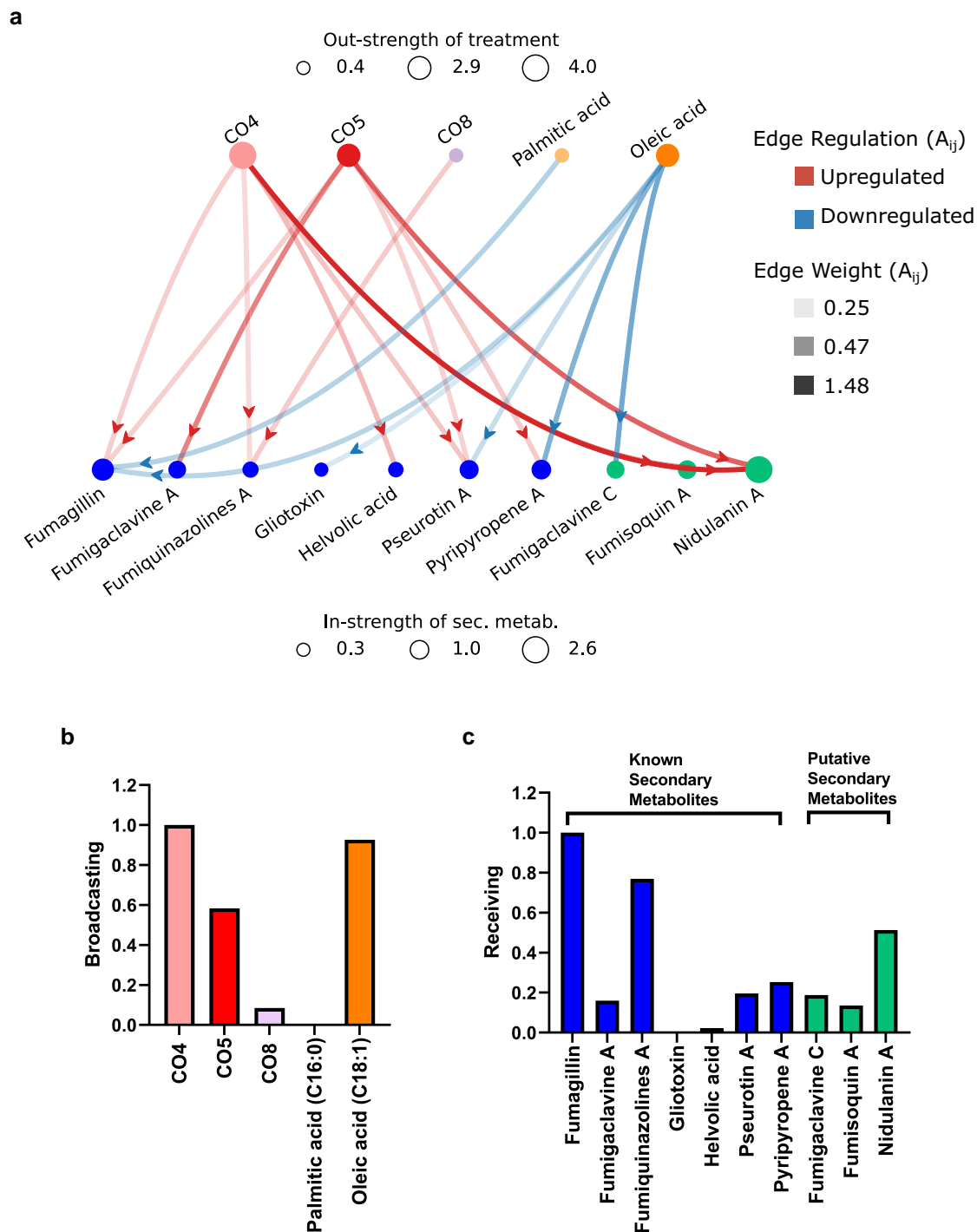


Fig. 4. Network analysis-based direct route for revealing the relationship between treatments and metabolite production in *A. fumigatus* at 25°C. (a) Bipartite network of treatments and known and putative metabolites. The nodes that represent the metabolites are classified and color coded as blue and green circles for known and putative metabolites (also denoted in (c)), respectively. The transparency and color (red or blue) of the edges represent the \log_2 fold change and up- or downregulation of the metabolites, respectively. CO4, CO5, and CO8 adjacent edges are up regulated. Palmitic and oleic acid adjacent edges are down regulated. The sizes of the nodes denote the network centrality measure of node strength. (b) Network centrality measure of PageRank of the treatments (broadcasting PageRank values). (c) PageRank measures of the known and putative metabolites (receiving PageRank values).

Comparison of the direct route to the traditional comparison methods at 37°C

The traditional comparison methods ranked CO4, CO5, CO8, palmitic acid, and then oleic acid from the highest to the lowest influence on analyte production (Fig. 3a). Moreover, the metabolites consistently found were fumagillin, fumiquinazolines F, and

pyripyropene A (Fig. 3b–f). The direct route revealed that palmitic acid was the treatment with the highest impact on metabolite production despite having the second-lowest set size in the UpSet plot (Fig. 3a). Moreover, palmitic acid appeared to significantly influence the output of fumagillin at this temperature (Fig. 5b and c). This is notable because we could show that at 25°C, palmitic

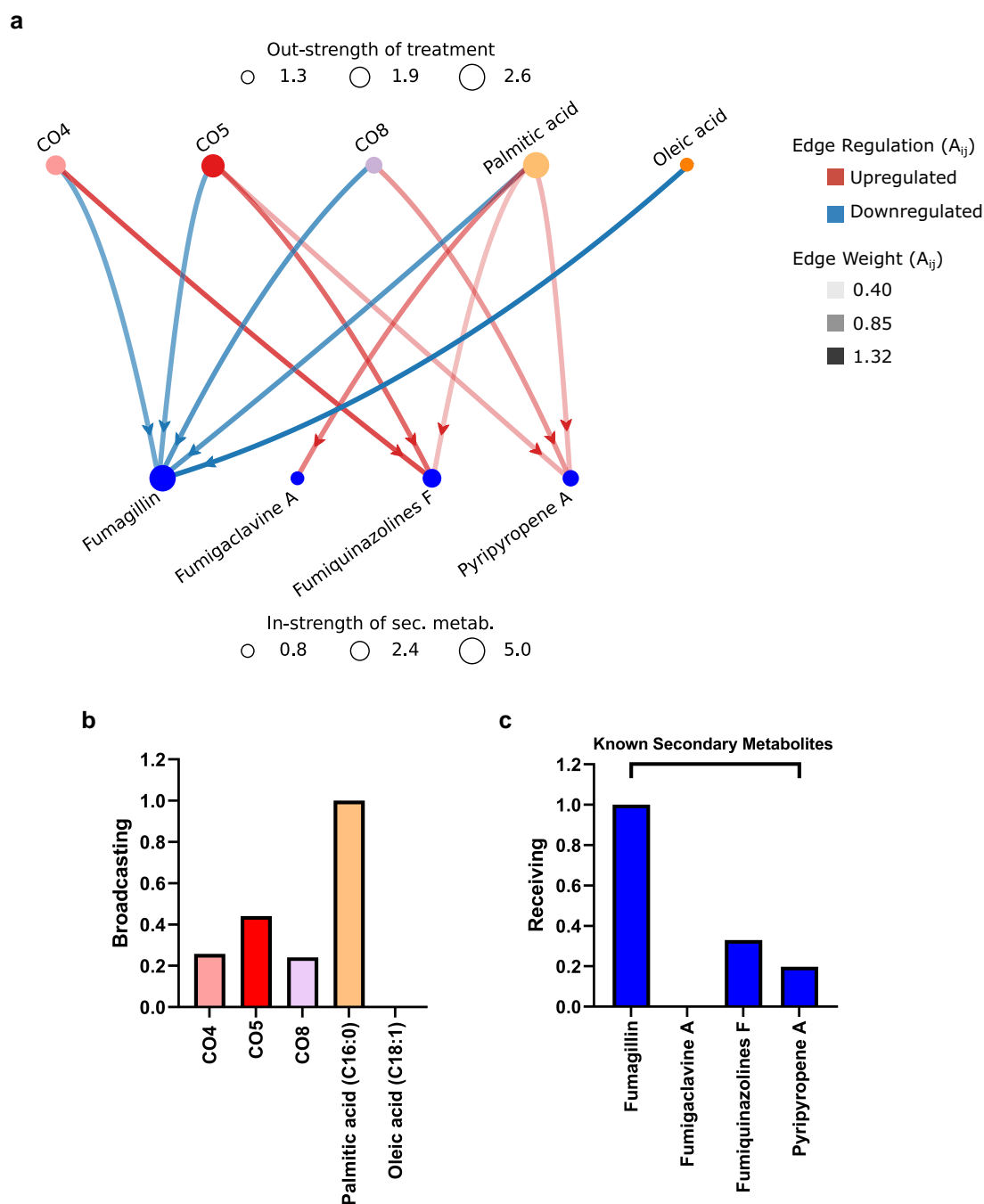


Fig. 5. Network analysis-based direct route for revealing the relationship between treatments and metabolite production in *A. fumigatus* at 37°C. (a) Bipartite network of treatments and known and putative metabolites. The nodes that represent the metabolites are classified and colored coded as blue circles for known metabolites (also denoted in (c)). The transparency and color (red or blue) of the edges represent the \log_2 fold change and up- or downregulation of the metabolites, respectively. Fumagillin adjacent edges are downregulated. Fumigaclavine A, fumiquinazolines F, and pyripyropene A are upregulated. The sizes of the nodes denote the network centrality measure of node strength. (b) Network centrality measure of PageRank of the treatments (broadcasting PageRank values). (c) PageRank measures of the known and putative metabolites (receiving PageRank values).

acid had negligible influence in eliciting any metabolite, but it is very active at higher temperatures. Other treatments that had significant influence at 25°C were impacted by the change in temperature, which resulted in less influence in eliciting metabolite production. Also, the direct route showed that fumagillin is a dominant metabolite produced by *A. fumigatus* regardless of treatments or temperature conditions. The importance and biological role of fumagillin from *A. fumigatus* is well documented (52). Because palmitic acid elicited production of fumagillin at 37°C, this raises an interesting question about the fungal impact on

human disease given that palmitic acid represents 20–30% of fatty acids in the human body (53) and fumagillin can lead to lung epithelial cell damage (54). Another difference between the temperatures was that COs-induced fumagillin production at 25°C, whereas an opposite regulation was observed at 37°C.

Summary of results from direct route

The results of the direct route revealed that CO4, and then oleic acid are the most dominant treatments that trigger a broad range of known and putative metabolites at 25°C. However, at 37°C,

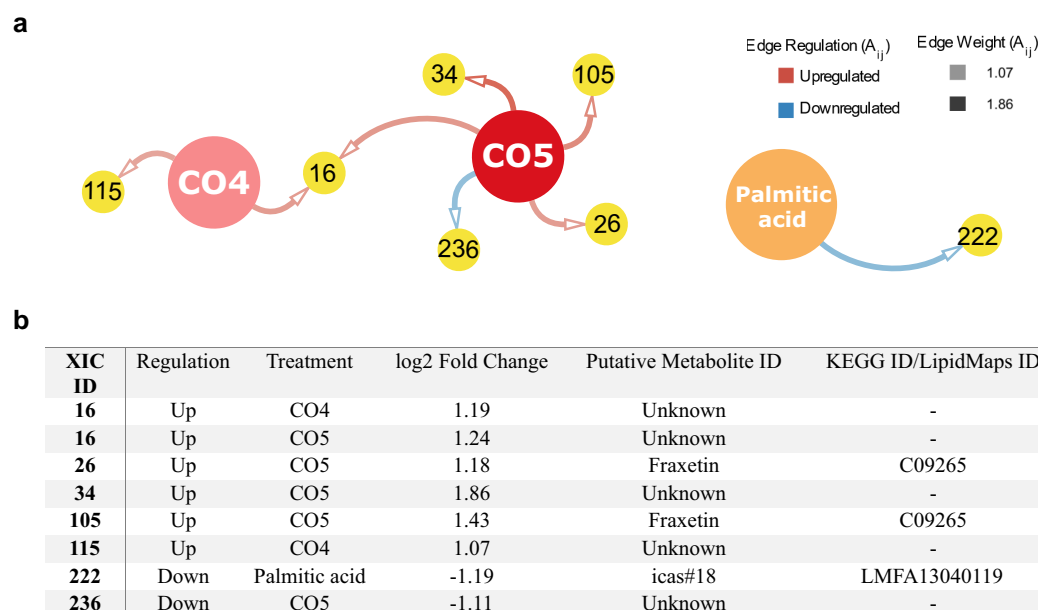


Fig. 6. Network analysis-based auxiliary route for revealing the relationship between treatments and metabolite production in *A. fumigatus* at 25°C. (a) Auxiliary route to assess the production of unknown analytes. A bipartite network of all analytes for their treatments (analyte IDs correspond to tables in [Online Supplementary Table S1](#) that provide mass-to-charge ratios (m/z), retention times, linear fold change, log₂ fold change, P -values, and f -values). The weights and colors (red and blue) of the edges illustrate the log₂ fold change of up- and downregulation (also listed in (b)) triggered by the treatments compared to the solvent control. (b) Table of putative metabolites produced at 25°C identified by the auxiliary route.

palmitic acid is the most effective treatment for metabolite production. We also found that fumagillin is the most receptive specialized metabolite in *A. fumigatus* to be triggered by various COs and lipids at both temperatures. For putative metabolite discovery, using network-based measures such as PageRank indicate that nidulanin A is the most receptive specialized metabolite triggered by COs and lipids at a lower temperature. Although nidulanin A production by *A. fumigatus* must be validated through gene knockout experiments, providing information about treatments that can trigger its production could help characterize it. Last, many of these known and putative metabolite peaks might still fall into a peak noise. Although a peak cutoff was initially used in MAVEN to identify bona fide peaks, the auxiliary route is used to identify known and unknown analytes or metabolites produced in response to a particular treatment by using an untargeted metabolomics approach.

Auxiliary route reveals the dominant compounds and highly influenced unknown analytes

Curation of mass spectra profiles

The auxiliary route follows an untargeted metabolomic profiling of the exogenous treatments' effects on metabolomic production. The results of the auxiliary route illustrated in Fig. 6a and listed in Fig. 6b demonstrates our ability to potentially isolate highly produced, known and unknown analytes that exhibit a log₂ fold change greater than 1.0 or less than -1.0 for future experimentation and characterization. In the direct route, we had a peak area cutoff of 5×10^5 to detect signals with significant peaks between a treatment and solvent control. This allowed for the identification and confirmation of known metabolites. Although our peak area cutoff of 5×10^5 eliminates most noise, it is a linear cutoff and leaves some residual noise (caused by column creep) in the analysis. Therefore, we first curated the dataset for the auxiliary route from the experimental study by using baseline correction preprocessing tools. [Online Supplementary Fig. S13](#) shows the

elimination of column creep and a new peak area cutoff suggested by Treviño et al. (55). To ensure the smallest amount of noise within our data, peak picking for our untargeted approach was conducted with GridMass (55) peak detection with a conservative threshold for peaks; no peaks under 3×10^7 were considered. Peaks were aligned by using RANSAC alignment. Peak data were then matched to known profiles in KEGG and LipidMap (16–19). Peak significance was determined by FCROS scoring (56). Nonsignificant analytes were not included in the network. [Online Supplementary Material A](#) provides additional details about the data curation for building the bipartite networks for the auxiliary route. The untargeted extraction of statistically relevant peaks by using the auxiliary route can yield a significant number of analytes for potential exploration. The edges and neighbors of the nodes in the network can be used to determine which analytes should be considered first for targeted exploration. Analytes of particular interest express both regulation and control depending on the treatment considered. Additionally, analytes of extreme up- and downregulation can be of interest along with the node degree values of the analytes.

Results at 25°C

A network of all significant peaks (i.e. all significant metabolites regardless of log₂ fold change intensity) is provided in [Online Supplementary Material B \(Fig. S14\)](#). Figure 6a only illustrates the significant peaks with a log₂ fold change greater than 1.0 or less than -1.0. The total number of interactions (edges in the network) found with the auxiliary route is considerably higher than with the network in the direct route. Thus, the auxiliary route reveals more information about the interactions among the exogenous treatments and metabolites than the direct route. Interesting artifacts are revealed from the network built using data at 25°C (Fig. 6b). We found seven unique extracted ion chromatograms (XICs) defined by their m/z , retention time, and area under the curve. XIC IDs 26 and 105 were matched to a fraxetin-like

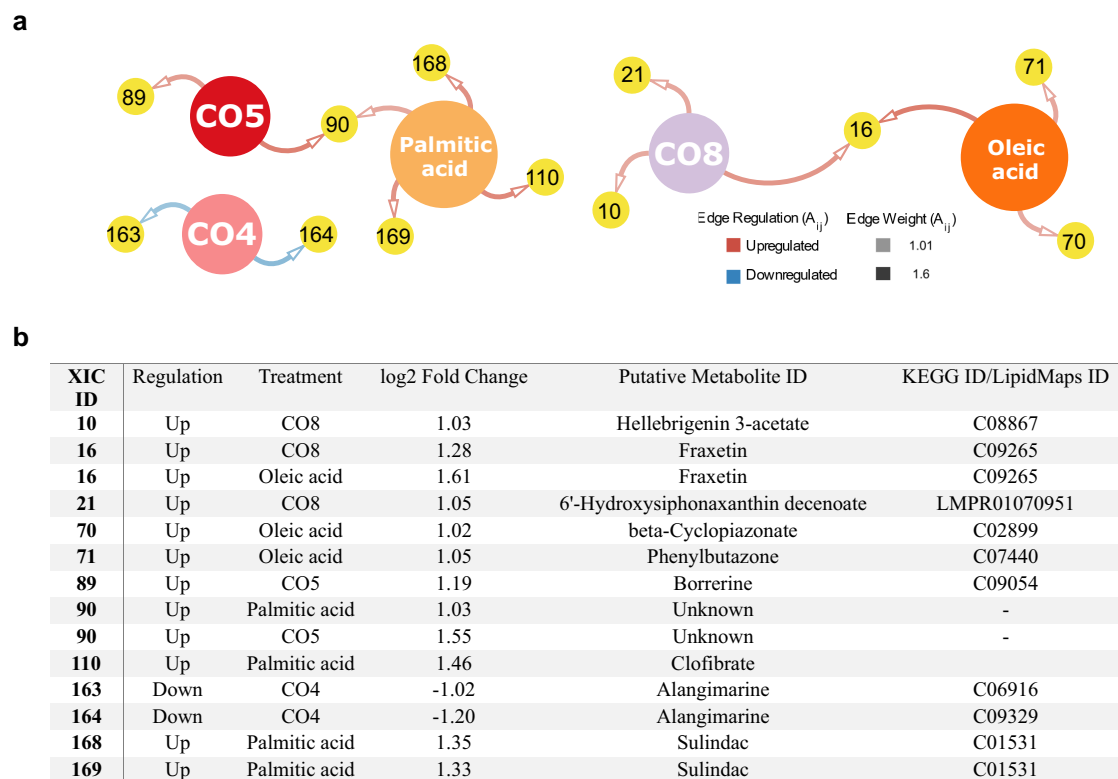


Fig. 7. Network analysis-based auxiliary route for revealing the relationship between treatments and metabolite production in *A. fumigatus* at 37°C. (a) Auxiliary route to assess the production of unknown analytes. A bipartite network of all analytes for their treatments (analyte IDs correspond to [Online Supplementary Table S2](#), which provides *m/z* values, retention times, linear fold change, log₂ fold change, *P*-values, and *f*-values). The weights and colors (red and blue) of the edges illustrate significant up- and downregulation (also listed in (b)) triggered by the treatments compared to the solvent control. (b) Table of putative metabolites produced at 37°C identified by the auxiliary route.

molecule via the KEGG database query, and they were upregulated when exposed to the CO5 treatment. Fraxetin was recently isolated from *A. fumigatus* and has an antibacterial activity (57). XIC ID 222 was matched to icas#18 (from the LipidMap database), which is a metabolite from the nematode *Caenorhabditis elegans* (58). Palmitic acid significantly downregulated icas#18 compared to the control. At the same time, no single highly produced analyte is triggered by all three COs. XIC ID 16 is an unknown analyte that is significantly produced and upregulated by both CO4 and CO5 treatments, thereby indicating that they might share a similar regulatory pathway to produce this unknown metabolite. Oddly, CO8 and oleic acid had no influence on analyte production with our log₂ fold change cutoff criteria. Notably, we found that several treatments had regulated the production of the same predicted analyte. These findings suggest that although treatments can commonly start the production of the analytes considered, the treatments used in the current study have a higher tendency to uniquely trigger analytes.

Analytes that immediately spark interest are the four unknown analytes: XIC IDs 16, 34, 115, and 236. Additional analytes of interest are those with opposing log₂ fold changes between treatments, whereas all remaining analytes within the networks have aligned log₂ fold changes. Although we do not see analytes with opposing log₂ fold changes in the network with all log₂ fold changes greater than 1.0 or less than -1.0 (Fig. 6a), we do see analytes with opposing log₂ fold change intensities with XIC IDs 13, 35, 115, and 188 ([Online Supplementary Fig. S14](#)) when considering all edges. A detailed discussion of the findings from the full data can be found in [Online Supplementary Material B](#).

Finally, we can validate our prediction by using the auxiliary route based on the confirmation of fraxetin production from a different study (57), in silico spiking and fragmentation patterns of fumigaclavine A ([Fig. S4](#) and [Online Supplementary Table S1](#)), and fragmentation pattern matches to public databases of fumi-quinazolines F ([Fig. S6](#) and [Online Supplementary Table S1](#)). Fumigaclavine A and fumi-quinazolines F were not within the threshold to be included in [Fig. 6b](#); instead, they are listed in [Online Supplementary Table S1](#).

Results at 37°C

Considering the analytes from the network at 37°C shown in [Fig. 7a](#), 12 significant analyte peaks with log₂ fold change intensities greater than 1.0 or less than -1.0 were extracted from the processed data. There were no commonly triggered XICs among the three COs or two lipids. From the 12 significant extracted analyte peaks, 11 were identified from database queries and defined as *like-compounds* because we did not confirm their identity through fragmentation patterns or comparison with a commercially available standard ([Fig. 7b](#)). Hellebrigenin 3-acetate (XIC ID 10) is a natural product isolated from the plants *Bersama abyssinica* (59) and *Kalanchoe spp.* (60) with no reported biological roles. Beta-cyclopiazonate (XIC ID 70) is a polyketide involved in the synthesis of cyclopiazonic acid, which is a mycotoxin produced by species of *Aspergillus* and *Penicillium* (61). Phenylbutazone is a synthesized molecule and anti-inflammatory drug (PubChem 4781). Borrerine (XIC ID 89) is an alkaloid identified from the plant

Table 1. Comparison of relevant capabilities of state-of-the-art metabolic network analysis tools (GNPS (21), MetWork (13), and MetaboAnalyst (32)) with the current approach.

Tool capability	Current method	State-of-the-art tools (13, 21, 32)	New contribution by current method
Network node definition	Analytes/metabolites and exogenous treatments	Analytes/metabolites	Yes
Network edge definition	Amount of analyte/metabolite triggered by a treatment	Spectral matching	Yes
Direction on network edges	Yes	No	Yes
Influence of treatment	Yes	No	Yes
Dominant triggers of metabolites	Yes	No	Yes
Network metrics to rank nodes	Yes	Yes	No
Discovering new compounds	Yes ^a	Yes	No

^aPutative IDs must be confirmed through fragmentation patterns or comparison to a commercially available standard (not performed in this study).

Borreria verticillata (62), which is reported to have antimicrobial activity (63), and has not been reported as a compound isolated from fungi. Clofibrate (XIC ID 110) is a synthesized molecule that plays a role as an anticholesteremic drug (64). Alangimarine (XIC IDs 163 and 164) is an isoquinoline alkaloid plant metabolite isolated from *Alangium lamarckii* (65). Sulindac (XIC IDs 168 and 169) is a nonsteroidal anti-inflammatory drug that is functionally related to an acetic acid (PubChem 1548887). The 6'-hydroxysiphonaxanthin decenoate (XIC ID 21) is a carotenoid described from green alga (66). Fraxetin, as in the 25°C results, was also identified, thereby indicating that this molecule may not be temperature dependent. The only unidentified analyte was XIC ID 90, which was upregulated in both CO5 and palmitic acid treatments. The regulated XIC IDs not within our log₂ fold change threshold are listed in [Online Supplementary Table S2](#).

When considering all analytes (not only those with log₂ fold changes greater than 1.0 or less than -1.0 as shown in [Fig. S15 in Online Supplementary Material B](#)), five analytes with opposing log₂ fold changes (analytes with XIC IDs 21, 70, 163, 164, and 168) were identified compared to the four analytes at 25°C. Analytes 163 and 168 were induced by three separate treatments. Analyte 163 is upregulated by both palmitic acid and CO8 and downregulated by CO4. Analyte 168 is upregulated by palmitic acid and downregulated by both CO4 and oleic acid.

Reportedly, oleic acid-induced germination in *A. fumigatus* at 37°C (40). To our knowledge, none of the known metabolites identified were previously linked to germination in *A. fumigatus*. Therefore, we are curious if one of the highly upregulated, unknown analytes could cause increased germination of this fungus at 37°C and could therefore be a target for future experiments. A detailed discussion of the findings from the full data can be found in [Online Supplementary Material B](#). Compared with the putative metabolites identified between to the two temperature conditions, there were metabolites expressed in our analysis at 37°C than at 25°C. Additionally, we validated our predictions the same way for all 25°C and 37°C samples. Finally, for metabolites derived from plants, it is unknown if those plants were colonized by fungi, and it is plausible that these putative XIC IDs are fungal metabolites.

Summary of results from auxiliary route

The results of the auxiliary route show that there are many more analytes produced than the current number of known and putative metabolites. The significant analytes extracted at temperatures 25 and 37°C comport not only with known and putative specialized metabolites but also with the rates at which the triggering of specialized metabolites have been witnessed in the previously discussed direct route. Moreover, new relationships among treatments and metabolites were revealed because all

found peak signals are considered in the auxiliary route. Of the significant analytes produced, there is a tremendous overlap in the activation of analyte production between treatments. Additionally, we found that by thresholding the edges at greater than or equal to 1 log₂ fold change, we could effectively illustrate how these treatments begin to interact with the up- and downregulation of the untargeted analytes. When considering all significant analytes, we see that within the 25°C network, the lipid treatments tend toward downregulation, whereas the COs tend to upregulate analyte production. Conversely, within the 37°C networks, we see that all treatments tend toward upregulation of analytes except for CO4, which has a relatively balanced amount of up- and downregulated-induced analytes.

Discussion and conclusion

The effects of compounds such as chitin and lipids on microbial metabolomic profiles are not fully elucidated and remain challenging to interpret. This study provides a data-driven modeling framework that uses network analysis to dissect the connection between exogenous inputs (e.g. biological compounds such as lipids and COs) and the metabolomic outputs (e.g. putative metabolites and unknown analytes) in the opportunistic human pathogen *A. fumigatus*. Bipartite networks with two classifications of nodes were built. The network nodes represent the treatments and specialized metabolites under consideration. The edges that connect the nodes represent the magnitude of up- or downregulation of the specialized metabolites triggered by the corresponding treatments. We provided two routes to characterize the production of the specialized metabolites: (1) the direct route for the production of known and putative metabolites and (2) the auxiliary route for the production of unknown analytes. Moreover, we used network centrality measures of node strength and PageRank to rank the treatments and specialized metabolites. The treatments are ranked based on their ability to trigger the production of various specialized metabolites. The specialized metabolites are ranked based on their ability to be influenced by multiple treatments.

Table 1 summarizes and compares the capabilities of the current framework with that of other state-of-the-art metabolic network analysis tools. Notably, although the referenced tools have a vast array of capabilities, we are only mentioning the ones that are relevant to the current analysis. Below, we state the new contributions from our methodology compared to the state-of-the-art tools:

- The network definition for representing interaction between exogenous treatments and metabolites is defined by the amount of regulation triggered by the treatments.

- Our network definition results in directed weighted networks, which differs from the binary undirected networks that are typically used in metabolomic networks in the literature.
- Our network can quantify the effect of exogenous treatments on metabolites.
- Our network can identify the most influential treatments and influenced metabolites to aid postprocessing applications for cost-effective drug discovery.

Some components of the method are based on previous knowledge:

- The concept of network (graph) theory (34) and metabolic networks (29, 35, 36).
- The network centrality metrics node strength (67) and PageRank (37).

Insights about the most effective treatments and most influenced specialized metabolites are valuable for (1) validating known specialized metabolites through applied exogenous treatments or environmental cues and (2) discovering new specialized metabolites from putative metabolites and unknown analytes by genetic knockouts to characterize their gene clusters, as depicted in postanalysis applications (Fig. 1). Ultimately, our goal was to track how a treatment elucidates the production of secondary metabolites. Most biosynthetic gene clusters are silent under standard culture conditions, and this results in minimal production of secondary metabolites. Our study can help researchers determine how their treatments or environmental conditions will improve the production and accumulation of natural products. Those results can be validated through mass spectrometry analysis and comparison to fragmentation patterns from published datasets or commercial standards and through transcriptomic analysis to assess their biosynthetic gene expressions. Further confirmation can be obtained through knockout experiments and functional validation of the targeted biosynthetic gene clusters in postanalysis applications, but that is outside the scope of the present work. This pilot study is our first approach to provide guidance for the metabolomic abyss, and, undoubtedly, future research can help improve the methods we have outlined here.

The cost of drug discovery can be exponential if experiments are designed as trial-and-error approaches. We provide a potentially cost-effective solution through direct and auxiliary routes (along with relevant codes for researchers to use on publicly available or newly generated LC-MS datasets). The inferences obtained from our framework can be used as a guide for industry partners and researchers to concentrate their efforts on natural product discovery and postanalysis applications for the most influential microbial metabolites and treatments.

Acknowledgments

We thank Sam Crawford for the careful editing of the text.

Supplementary material

Supplementary material is available at PNAS Nexus online.

Funding

This research used resources of the Oak Ridge Leadership Computing Facility at the Oak Ridge National Laboratory, which

is supported by the Office of Science of the U.S. Department of Energy (DOE) under Contract No. DE-AC05-00OR22725. This research was also funded by the Genomic System Sciences Program, U.S. Department of Energy, Office of Science, Biological and Environmental Research, as part of the Plant-Microbe Interfaces Scientific Focus Area at the Oak Ridge National Laboratory (<http://pmi.ornl.gov>). Figure 1 was created and edited with BioRender. The U.S. government retains and the publisher, by accepting the article for publication, acknowledges that the U.S. government retains a nonexclusive, paid-up, irrevocable, worldwide license to publish or reproduce the published form of this manuscript, or allow others to do so, for U.S. government purposes. DOE will provide public access to these results of federally sponsored research in accordance with the DOE Public Access Plan (<http://energy.gov/downloads/doe-public-access-plan>).

Author contributions

M.G.M., M.J.L., J.T., and T.A.R. initiated and designed the project. J.-M.A. and J.L.L. provided the COs and lipids. N.P.K. provided *A. fumigatus* strain Af293. T.A.R., J.T., and A.A.C. designed and implemented the experiments with *A. fumigatus*. M.G.M. designed and conducted the direct route. M.J.L., D.K., and D.A.J. conducted the auxiliary route. P.E.A., R.J.G., J.T., and T.A.R. conducted and analyzed the mass spectrometry datasets. M.G.M., M.J.L., J.T., and T.A.R. wrote the manuscript with feedback from all coauthors. A.G.G. contributed analytic tools and provided feedback on the text.

Preprints

This manuscript was posted on a preprint: <https://doi.org/10.1101/2022.08.11.503656>.

Data availability

Correspondence and requests for material should be addressed to M.G.M or T.A.R. The codes are available for academic or commercial use. Please reach out to the authors or partnerships@ornl.gov. All LC-MS raw data files used in this study were deposited at the Massive repository (<https://massive.ucsd.edu/ProteoSFAfe/static/massive.jsp>). The metadata can be accessed using the dataset ID: MSV000090575 and password: LIPIDSCO (or use the FTP link <ftp://MSV000090575@massive.ucsd.edu>).

Network illustrations and web based interactive networks for the auxiliary route were generated using Cytoscape (version 3.9.1). The interactive networks can be found at <https://doi.org/10.5281/zenodo.8401025>. For each analysis (25 or 37°C), please browse through the different individual networks of the treatments and the full network, union, by using the Network tab. Click the Show/Hide Table tool on the right-hand side tool bar and click a node (treatment or analyte) or edge on the network to show full characteristics.

References

- 1 Keller NP. 2019. Fungal secondary metabolism: regulation, function and drug discovery. *Nat Rev Microbiol.* 17(3):167–180.
- 2 Keller NP, Turner G, Bennett JW. 2005. Fungal secondary metabolism—from biochemistry to genomics. *Nat Rev Microbiol.* 3(12):937–947.
- 3 Nickles GR, Oestereicher B, Keller NP, Drott M. 2023. Mining for a new class of fungal natural products: the evolution, diversity,

- and distribution of isocyanide synthase biosynthetic gene clusters. *Nucleic Acids Res.* 51(14):7220–7235.
- 4 Gerke J, Braus GH. 2014. Manipulation of fungal development as source of novel secondary metabolites for biotechnology. *Appl Microbiol Biotechnol.* 98(20):8443–8455.
 - 5 Newman DJ, Cragg GM. 2020. Natural products as sources of new drugs over the nearly four decades from 01/1981 to 09/2019. *J Nat Prod.* 83(3):770–803.
 - 6 Boruta T. 2018. Uncovering the repertoire of fungal secondary metabolites: from Fleming's laboratory to the international space station. *Bioengineered.* 9(1):12–16.
 - 7 Naranjo-Ortiz MA, Gabaldón T. 2019. Fungal evolution: diversity, taxonomy and phylogeny of the Fungi. *Biol Rev.* 94(6):2101–2137.
 - 8 Robey MT, Caesar LK, Drott MT, Keller NP, Kelleher NL. 2021. An interpreted atlas of biosynthetic gene clusters from 1,000 fungal genomes. *Proc Natl Acad Sci USA.* 118(19):e2020230118.
 - 9 Brakhage AA, Schroeckh V. 2011. Fungal secondary metabolites—strategies to activate silent gene clusters. *Fungal Genet Biol.* 48(1):15–22.
 - 10 Blin K, et al. 2023. Antismash 7.0: new and improved predictions for detection, regulation, chemical structures and visualisation. *Nucleic Acids Res.* 51(W1):W46–W50.
 - 11 Blin K, et al. 2021. Antismash 6.0: improving cluster detection and comparison capabilities. *Nucleic Acids Res.* 49(W1):W29–W35.
 - 12 Blin K, et al. 2019. Antismash 5.0: updates to the secondary metabolite genome mining pipeline. *Nucleic Acids Res.* 47(W1):W81–W87.
 - 13 Beauvais Y, Genta-Jouve G. 2019. Metwork: a web server for natural products anticipation. *Bioinformatics.* 35(10):1795–1796.
 - 14 Clasquin MF, Melamud E, Rabinowitz JD. 2012. LC-MS data processing with maven: a metabolomic analysis and visualization engine. *Curr Protoc Bioinformatics.* 37(1):14–11.
 - 15 Domingo-Almenara X, Siuzdak G. 2020. Metabolomics data processing using xcms. In: Li S, editor. *Computational methods and data analysis for metabolomics.* Humana, New York, NY: Springer. p. 11–24.
 - 16 Fahy E, et al. 2009. Update of the LIPID MAPS comprehensive classification system for lipids. *J Lipid Res.* 50(Suppl.):S9–14.
 - 17 Kanehisa M. 2019. Toward understanding the origin and evolution of cellular organisms. *Protein Sci.* 28(11):1947–1951.
 - 18 Kanehisa M, Furumichi M, Sato Y, Ishiguro-Watanabe M, Tanabe M. 2020. KEGG: integrating viruses and cellular organisms. *Nucleic Acids Res.* 49(D1):D545–D551.
 - 19 Kanehisa M, Goto S. 2000. KEGG: kyoto encyclopedia of genes and genomes. *Nucleic Acids Res.* 28(1):27–30.
 - 20 Melamud E, Vastag L, Rabinowitz JD. 2010. Metabolomic analysis and visualization engine for LC-MS data. *Anal Chem.* 82(23):9818–9826.
 - 21 Wang M, et al. 2016. Sharing and community curation of mass spectrometry data with global natural products social molecular networking. *Nat Biotechnol.* 34(8):828–837.
 - 22 Wang X, Subko K, Kildgaard S, Frisvad JC, Larsen TO. 2021. Mass spectrometry-based network analysis reveals new insights into the chemodiversity of 28 species in *Aspergillus* section *Flavi*. *Front Fungal Biol.* 2:32.
 - 23 Nickles G, Ludwikowski I, Bok JW, Keller NP. 2021. Comprehensive guide to extracting and expressing fungal secondary metabolites with *Aspergillus fumigatus* as a case study. *Curr Protoc.* 1(12):e321.
 - 24 Tannous J, Labbé J, Keller NP. 2023. Identifying fungal secondary metabolites and their role in plant pathogenesis. In: Foroud NA, Neilson JAD, editors. *Plant–pathogen interactions.* p. 193–218. Humana, New York, NY: Springer.
 - 25 Rush TA. 2021. Bioprospecting trichoderma: a systematic roadmap to screen genomes and natural products for biocontrol applications. *Front Fungal Biol.* 2:41.
 - 26 Lind AL, Smith TD, Saterlee T, Calvo AM, Rokas A. 2016. Regulation of secondary metabolism by the velvet complex is temperature-responsive in *Aspergillus*. *G3: Genes, Genomes, Genetics.* 6(12):4023–4033.
 - 27 Losada L, Ajayi O, Frisvad JC, Yu J, Nierman WC. 2009. Effect of competition on the production and activity of secondary metabolites in *Aspergillus* species. *Med Mycol.* 47(Suppl. 1):S88–S96.
 - 28 Pfannenstiel BT, Keller NP. 2019. On top of biosynthetic gene clusters: how epigenetic machinery influences secondary metabolism in fungi. *Biotechnol Adv.* 37(6):107345.
 - 29 Newman M. 2018. *Networks.* Oxford University Press.
 - 30 Rush TA, et al. 2022. Lipo-chitooligosaccharides induce specialized fungal metabolite profiles that modulate bacterial growth. *Msystems.* 7(6):e01052–22.
 - 31 Pang Z, et al. 2021. Metaboanalyst 5.0: narrowing the gap between raw spectra and functional insights. *Nucleic Acids Res.* 49(W1):W388–W396.
 - 32 Xia J, Psychogios N, Young N, Wishart DS. 2009. Metaboanalyst: a web server for metabolomic data analysis and interpretation. *Nucleic Acids Res.* 37(Suppl. 2):W652–W660.
 - 33 Bandeira N, Tsur D, Frank A, Pevzner PA. 2007. Protein identification by spectral networks analysis. *Proc Natl Acad Sci USA.* 104(15):6140–6145.
 - 34 Bollobás B. 1998. *Modern graph theory.* Springer.
 - 35 Jeong H, Tombor B, Albert R, Oltvai ZN, Barabási A-L. 2000. The large-scale organization of metabolic networks. *Nature.* 407(6804):651–654.
 - 36 Wagner A, Fell DA. 2001. The small world inside large metabolic networks. *Proc Royal Soc London Ser B Biol Sci.* 268(1478):1803–1810.
 - 37 Brin S, Page L. 1998. The anatomy of a large-scale hypertextual web search engine. *Comput Netw ISDN Syst.* 30(1–7):107–117.
 - 38 Crosino A, et al. 2021. Extraction of short chain chitooligosaccharides from fungal biomass and their use as promoters of arbuscular mycorrhizal symbiosis. *Sci Rep.* 11(1):1–12.
 - 39 Nemeč T, Jernejc K, Cimerman A. 1997. Sterols and fatty acids of different *Aspergillus* species. *FEMS Microbiol Lett.* 149(2):201–205.
 - 40 Rush TA, et al. 2020. Lipo-chitooligosaccharides as regulatory signals of fungal growth and development. *Nat Commun.* 11(1):1–10.
 - 41 Mellon JE, Cotty PJ, Dowd MK. 2000. Influence of lipids with and without other cottonseed reserve materials on aflatoxin B1 production by *Aspergillus flavus*. *J Agric Food Chem.* 48(8):3611–3615.
 - 42 Liaquat F, Eltem R. 2018. Chitooligosaccharides and their biological activities: a comprehensive review. *Carbohydr Polym.* 184:243–259.
 - 43 Raffa N, Keller NP. 2019. A call to arms: mustering secondary metabolites for success and survival of an opportunistic pathogen. *PLoS Pathog.* 15(4):e1007606.
 - 44 Berthier E, et al. 2013. Low-volume toolbox for the discovery of immunosuppressive fungal secondary metabolites. *PLoS Pathog.* 9(4):e1003289.
 - 45 Hagiwara D, et al. 2017. Temperature during conidiation affects stress tolerance, pigmentation, and trypacidin accumulation in the conidia of the airborne pathogen *Aspergillus fumigatus*. *PLoS ONE.* 12(5):e0177050.
 - 46 Kosalec I, Pepeljnjak S, Jandrič M. 2005. Influence of media and temperature on gliotoxin production in *Aspergillus fumigatus* strains. *Arh Hig Rada Toksikol.* 56(3):269–273.
 - 47 Nierman WC, et al. 2005. Genomic sequence of the pathogenic and allergenic filamentous fungus *Aspergillus fumigatus*. *Nature.* 438(7071):1151–1156.

- 48 Latgé J-P. 1999. *Aspergillus fumigatus* and aspergillosis. *Clin Microbiol Rev.* 12(2):310–350.
- 49 Croft CA, Culibrk L, Moore MM, Tebbutt SJ. 2016. Interactions of *Aspergillus fumigatus* conidia with airway epithelial cells: a critical review. *Front Microbiol.* 7:472.
- 50 Tannous J, et al. 2018. Fungal attack and host defence pathways unveiled in near-avirulent interactions of penicillium expansum creA mutants on apples. *Mol Plant Pathol.* 19(12):2635–2650.
- 51 Bignell E, Cairns TC, Throckmorton K, Nierman WC, Keller NP. 2016. Secondary metabolite arsenal of an opportunistic pathogenic fungus. *Philos Trans R Soc B Biol Sci.* 371(1709):20160023.
- 52 Guruceaga X, et al. 2019. Fumagillin, a mycotoxin of *Aspergillus fumigatus*: biosynthesis, biological activities, detection, and applications. *Toxins.* 12(1):7.
- 53 Carta G, Murru E, Banni S, Manca C. 2017. Palmitic acid: physiological role, metabolism and nutritional implications. *Front Physiol.* 8:902.
- 54 Chu SG, et al. 2019. Palmitic acid-rich high-fat diet exacerbates experimental pulmonary fibrosis by modulating endoplasmic reticulum stress. *Am J Respir Cell Mol Biol.* 61(6):737–746.
- 55 Treviño V, et al. 2015. Gridmass: a fast two-dimensional feature detection method for LC/MS. *J Mass Spectrom.* 50(1):165–174.
- 56 Dembélé D, Kastner P. 2014. Fold change rank ordering statistics: a new method for detecting differentially expressed genes. *BMC Bioinformatics.* 15(1):1–15.
- 57 Zihad S. 2022. Isolation and characterization of antibacterial compounds from *Aspergillus fumigatus*: an endophytic fungus from a mangrove plant of the Sundarbans. *Evid Based Complement Alternat Med.* 2022:9600079.
- 58 Von Reuss SH, et al. 2012. Comparative metabolomics reveals biogenesis of ascariosides, a modular library of small-molecule signals in *C. elegans*. *J Am Chem Soc.* 134(3):1817–1824.
- 59 Kupchan SM, Hemingway RJ, Hemingway JC. 1968. The isolation and characterization of hellebrigenin 3-acetate and hellebrigenin 3, 5-diacetate, bufadienolide tumor inhibitors from *Bersama abyssinica*. *Tetrahedron Lett.* 9(2):149–152.
- 60 Nascimento LBdS, Casanova LM, Costa SS. 2023. Bioactive compounds from *Kalanchoe* genus potentially useful for the development of new drugs. *Life.* 13(3):646.
- 61 Uka V, et al. 2017. Unravelling the diversity of the cyclopiazonic acid family of mycotoxins in *Aspergillus flavus* by UHPLC triple-TOF HRMS. *Toxins.* 9(1):35.
- 62 Pousset J-L, et al. 1973. La borreverine: nouvel alcaloïde isolé du *Borreria verticillata*. *Phytochemistry.* 12(9):2308–2310.
- 63 Pousset J-L, Cave A, Chiaroni A, Riche C. 1977. A novel bis-indole alkaloid. X-ray crystal structure determination of borreverine and its rearrangement product on diacetylation. *J Chem Soc Chem Commun.* 8:261–262.
- 64 Endo A. 2010. A historical perspective on the discovery of statins. *Proc Jpn Acad Ser B.* 86(5):484–493.
- 65 Pakrashi S, Achari B, Ali E, Dastidar PG, Sinha R. 1980. Novel benzopyridoquinolizine bases from *Alangium lamarckii* Thw. *Tetrahedron Lett.* 21(27):2667–2670.
- 66 Egeland ES, Guillard RR, Liaaen-Jensen S. 1997. Additional carotenoid prototype representatives and a general chemosystematic evaluation of carotenoids in Prasinophyceae (Chlorophyta). *Phytochemistry.* 44(6):1087–1097.
- 67 Barrat A, Barthélemy M, Pastor-Satorras R, Vespignani A. 2004. The architecture of complex weighted networks. *Proc Natl Acad Sci USA.* 101(11):3747–3752.